Clinical Imaging 47 (2018) 90–95

Contents lists available at ScienceDirect

Clinical Imaging

journal homepage: www.elsevier.com/locate/clinimag

Original Article

Apparent diffusion coefficient in the analysis of prostate cancer: determination of optimal b-value pair to differentiate normal from malignant tissue

Nuno Adubeiro[a,b,*], Maria Luísa Nogueira[c], Rita G. Nunes[d], Hugo Alexandre Ferreira[e], Eduardo Ribeiro[f,g], José Maria Ferreira La Fuente[h,i]

[a] Institute of Biomedical Sciences Abel Salazar (ICBAS), University of Porto, Rua de Jorge Viterbo Ferreira, 228, 4050-313 Porto, Portugal
[b] Department of Radiology, School of Health of Porto/Polytechnic Institute of Porto (ESS/IPP), Rua Dr. António Bernardino de Almeida 400, 4200-072 Porto, Portugal
[c] Department of Radiology, School of Health of Porto/Polytechnic Institute of Porto (ESS/IPP), Rua Dr. António Bernardino de Almeida 400, 4200-072 Porto, Portugal
[d] Institute for Systems and Robotics and Department of Bioengineering, LARSyS, Instituto Superior Técnico, Universidade de Lisboa, Av. Rovisco Pais 1, 1049-001 Lisboa, Portugal
[e] Institute of Biophysics and Biomedical Engineering (IBEB), Faculty of Sciences, University of Lisbon, Campo Grande, 1749-016 Lisboa, Portugal
[f] Department of Radiology, MRI Unit, Centro Hospitalar do Porto, Largo Prof. Abel Salazar, 4099-001 Porto, Portugal
[g] Department of Radiology, School of Health of Porto (ESS), Rua Dr. António Bernardino de Almeida 400, 4200-072 Porto, Portugal
[h] Institute of Biomedical Sciences Abel Salazar (ICBAS), University of Porto, Rua de Jorge Viterbo Ferreira, 228, 4050-313 Porto, Portugal.
[i] Department of Urology, Center Hospitalar Porto (CHP), Largo Prof. Abel Salazar, 4099-001 Porto, Portugal

ARTICLE INFO

Keywords:
ADC
B-value
Diffusion weighted imaging
Prostate cancer

ABSTRACT

Purpose: Determining optimal b-value pair for differentiation between normal and prostate cancer (PCa) tissues.
Methods: Forty-three patients with diagnosis or PCa symptoms were included. Apparent diffusion coefficient (ADC) was estimated using minimum and maximum b-values of 0, 50, 100, 150, 200, 500 s/mm2 and 500, 800, 1100, 1400, 1700 and 2000s/mm2, respectively. Diagnostic performances were evaluated when Area-under-the-curve (AUC) > 95%.
Results: 15 of the 35 b-values pair surpassed this AUC threshold. The pair (50, 2000 s/mm2) provided the highest AUC (96%) with ADC cutoff 0.89 × 10–^{3} mm^2/s, sensitivity 95.5%, specificity 93.2% and accuracy 94.4%.
Conclusions: The best b-value pair was b = 50, 2000 s/mm2.

1. Introduction

Diagnosing prostate disease is a complex task and typically requires a combination of clinical, biochemical and imaging biomarkers [1,2]. Specifically, the diagnosis of prostate cancer (PCa) is based on clinical symptoms, digital rectal examination, prostate specific antigen (PSA) levels, transrectal ultrasonography (TRUS) and tissue sample biopsy guided by TRUS, from which histopathological tissues are graded using the Gleason Score (GS). Despite advances in these techniques, the accuracy of the tests remains limited, missing some PCa cases [3].

Multi-parametric magnetic resonance imaging (MP-MRI) can aid in the detection and characterization of PCa combining anatomical, functional and molecular imaging, providing improved support for decision-making regarding clinical treatment [4,5]. This MP-MRI approach includes the use of diffusion-weighted imaging (DWI) for studying the prostate. DWI provides qualitative and quantitative microstructural information, in a non-invasive manner, making use of water diffusion to probe prostatic tissue [6]. DWI measures the motion of water molecules within tissues, which is influenced by the presence of intra and extracellular compartments as well as intravascular spaces. The apparent diffusion coefficient (ADC) is a measure of water mobility and can be estimated from the signal intensity (SI) decay between two or more images exhibiting different levels of diffusion contrast (quantified by the b-value). Previous studies reported reduced ADC values in PCa compared to benign and healthy tissue [7,8]. In order for ADC quantification to become more widespread in the clinic, it is essential to standardize prostate DWI protocols. Several parameters influence both the acquisition time and the measured ADC values, impacting the accuracy of the technique; these include the repetition time (TR), the echo time (TE) and the number and the choice of b-values [7,9–11].

* Corresponding author at: School of Health of Porto/Polytechnic Institute of Porto (ESS/IPP), Rua Dr. António Bernardino de Almeida 400, 4200-072 Porto, Portugal; Institute of Biomedical Sciences Abel Salazar (ICBAS), University of Porto, Rua de Jorge Viterbo Ferreira, 228, 4050-313 Porto, Portugal.
E-mail address: nca@eu.ipp.pt (N. Adubeiro).

http://dx.doi.org/10.1016/j.clinimag.2017.09.004
Received 1 June 2017; Received in revised form 4 September 2017; Accepted 6 September 2017

To minimize scanning time, while maintaining the best possible diagnostic performance, the determination of an optimal pair of b-values is desirable. Choosing the maximum and minimum b-values for adequate ADC estimation thus becomes critical. Recent recommendations state that the minimum b-value should range between 50 and 100 s/mm^2, to reduce the impact of micro-perfusion in capillaries on the ADC estimate, while the maximum b-value should be chosen within the 800–1000 s/mm^2 interval [12]. However, it has been acknowledged that visual evaluation of DWI acquired with b-values higher than 1400 s/mm^2 can be advantageous due to improved lesion conspicuity [12]. Several studies have already explored pairs of b-values with maximum b-values beyond this limit for ADC quantification [7,8,10,11,13]. However, there is still no consensus regarding the optimal b-value pair at 3 T. A study by Wang et al. [11] at 3.0 T compared diagnostic performance for different maximum b-values, but selected a fixed minimum b-value of 0 s/mm^2, which is not in agreement with current guidelines [12].

At 1.5 T, Peng et al. [10] compared seven b-value pairs ranging from 0 to 2000 s/mm^2 obtaining an ADC cut-off of 1.44 × 10^{-3} mm^2/s, with the highest sensitivity (86.2%) and specificity (92.3%) for the b-value pair 0, 1000 s/mm^2. However, since the signal-to-noise ratio (SNR) of the images is dependent on the field strength, the role of higher b-values for ADC quantification needs to be reevaluated at 3 T.

The purpose of this study was therefore to evaluate the optimal pair of b-values for ADC estimation at 3.0 T, resulting in the best performance for differentiating healthy tissue from PCa.

2. Methods

2.1. Subjects and lesions

This prospective study was approved by the Hospital Ethics Committee (reference number 251/12(190-DEFI/195-CES)), and all patients gave written informed consent.

One-hundred consecutive male patients, referred to our institution from October 2013 to January 2015, with previous diagnosis or symptoms suggestive of PCa and clinical indication to perform pelvic MRI, were enrolled in the study. Exclusion criteria were: a) prior surgery, hormonal or radiation therapy before MP-MRI (n = 11); b) MP-MRI analysis without detected lesions (n = 19); c) absence of positive histological PCa results obtained up to 6 months from MRI examination (n = 24); and d) diffusion images with artifacts (n = 3). The final number of patients was reduced to 43 (average age of 63, age range: 45–76 years old). The pathologic confirmation of PCa was made by TRUS biopsy (n = 21) or prostatectomy (n = 22).

2.2. MR equipment and image acquisition protocol

Prostate MP-MRI was done using a 3 T MR scanner (Achieva TX with Multi Transmit technology, Philips Healthcare, Netherlands) equipped with a 32 channel phased-array coil. The MRI protocol included: T2-weighted (w) turbo spin-echo (TSE) sequence in the axial and coronal planes TR, 4000 ms; TE, 100 ms; thickness, 3 mm; matrix, 200 × 200; number of excitations (NEX) 2; scan time 1:12 min); sagittal T2-w TSE sequence (TR, 4000 ms; TE, 140 ms; thickness, 3.5 mm; matrix, 232 × 200; NEX 2; scan time 1:12 min); axial T1-w TSE sequence (TR, 589 ms; TE, 20 ms; thickness, 3.5 mm; matrix, 316 × 269; NEX 2; scan time 2:12 min); axial T2-w TSE sequence (TR, 4722 ms; TE, 140 ms; thickness, 3.5 mm; matrix, 432 × 400; NEX 2; scan time 2:40 min) with spectral pre-saturation with inversion recovery (SPIR); dynamic axial T1-w contrast-enhanced fast field echo (CE-FFE-T1) with fat saturation (TR, 6.4 ms; TE, 3.2 ms; thickness, 3 mm; matrix, 160 × 160; NEX 3; scan time 2:39 min). DWI was acquired before the dynamic sequence with a single-shot spin-echo echo-planar imaging (SS-SE-EPI) sequence with SPIR for fat suppression and parallel imaging. Sensitizing diffusion gradients were applied in the -x, -y and -z directions to generate 3-scan trace images with b-values of 0, 50, 100, 150, 200, 500, 800, 1100, 1400, 1700 and 2000 s/mm^2 (slice thickness 6 mm; TR 3258 ms; TE, 66 ms, matrix, 124 × 100, field-of-view 375 × 375 mm^2; NEX 2; scan time 13:21 min).

2.3. Data analysis

Prostate images were evaluated by a radiologist (with > 5 years of experience) who localized and described the lesions combining information from morphologic and dynamic images.

Taking into account the clinical imaging report, two radiology researchers, with training in DWI (both with over 5 years of experience), localized the lesions in the DW images. T1-w and T2-w images were evaluated to avoid areas of post-biopsy hemorrhage and ADC maps were generated to rule out T2-w shine-through effects. The slice that better depicted the lesion, corresponding to its highest dimension was chosen, accounting for the prostate sector identified by the prostatectomy or TRUS biopsy report.

Regions of interest (ROI) were drawn around the lesion encompassing the hyperintense region at b = 2000 s/mm^2 and copied to the other diffusion images. Regarding healthy glandular tissue, ROI were drawn in T2-w images with a fixed size of 21.75 mm^2 in the peripheral zone (PZ) and in the central gland (CG) and copied to the DW images. These images were then visualized so as to ensure that the ROI fell within the intended anatomical structure and did not exhibit hyperintense signal in b2000 s/mm^2. Furthermore, to avoid MRI-occult lesions, the histology reports were taken into account when delineating the ROI. Mean signal intensities (SI) for each DW image were recorded for both regions of healthy tissue and lesions.

ADC maps were generated for each b-value combination using the software *Osirix Dicom Viewer version 5.6.1*. with the equation [14]:

$$ADC = -\ln(SI_{b2}/SI_{b1})/(b2 - b1)$$

where SI_{b2} is the SI corresponding to the higher b-value $b2$, and SI_{b1} corresponded to the lower b-value $b1$.

The ADC was estimated using different combinations of minimum b-values of 0, 50, 100, 150, 200, 500 s/mm^2 and maximum b-values of 500, 800, 1100, 1400, 1700 and 2000 s/mm^2, resulting in thirty five studied b-value combinations (e.g. 0, 800; 0, 2000; 50, 1000; 100, 2000 s/mm^2 and so forth). The b-value combination 500,500 s/mm^2 was ruled out.

2.4. Statistical analysis and clinical validation

A descriptive analysis was performed for normal tissue and PCa. For each b-value combination, mean ADC values and standard deviations (SD) were computed for healthy tissue and malignant lesions.

For all the 35 b-value combinations, the area-under-the-curve (AUC) was estimated by receiver operating characteristics (ROC) analysis. The best pairs of b-values were identified as the combinations that showed AUC > 95%. The pairs of b-values that did not fulfill this criterion were excluded. For the best b-value pairs, ADC cut-off and diagnostic performance were calculated considering Youden statistics and the minimum distance between the ROC curve and the ideal point of coordinates (0, 1). AUC comparison for obtained ROC curves was done according to Delong et al. using MedCalc software version 17 (Medcalc Software, Ostend, Belgium) [15].

The Mann-Whitney test was used to evaluate differences between PCa and normal tissue, both globally and by region of lesion localization, for the best b-value combinations.

Overall differences in mean ADC values between the best b-value pairs were assessed, using the Friedman nonparametric repeated measures analysis of variance test.

The Statistical Package for the Social Sciences (SPSS) software version 20.0 was used for analysis and a p-value < 0.05 was considered statistically significant.

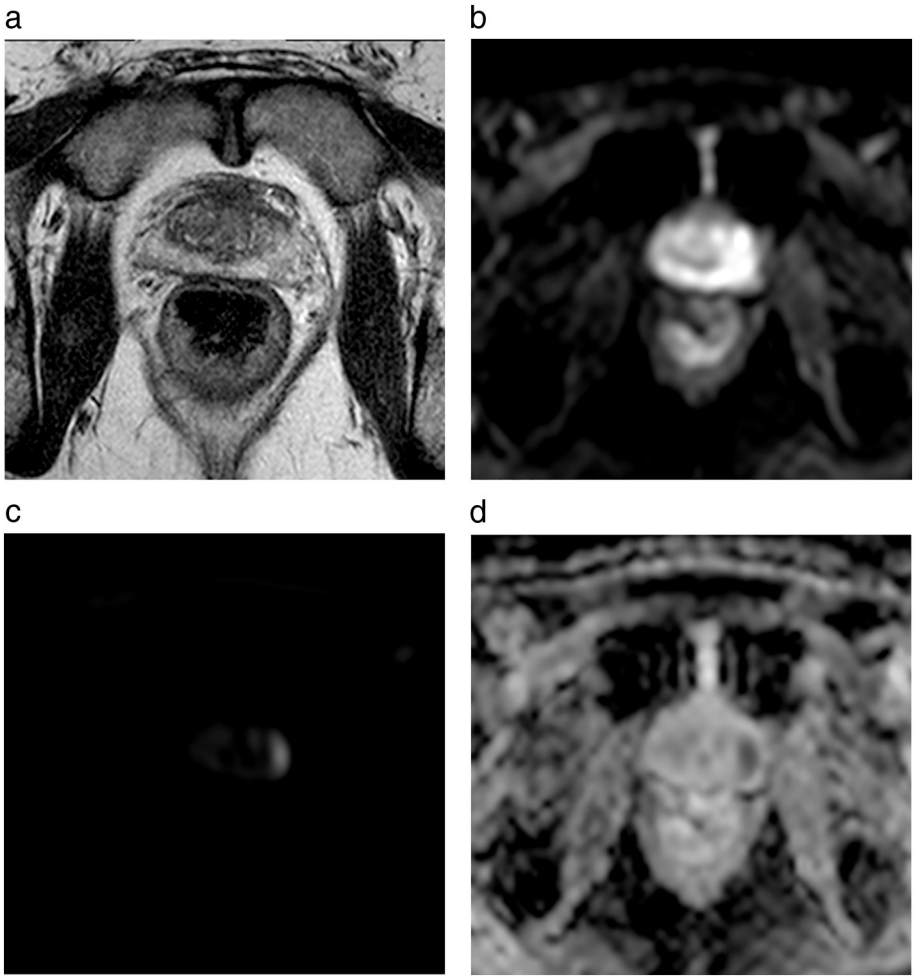

Fig. 1. A 65-years-old patient with PCa in the left PZ of the prostate. (a) T2-w image shows a hipointense signal area in the left PZ. (b) DW image with a b-value of 50 s/mm^2. (c) DW image with a b-value of 2000 s/mm^2 showing a hyperintense signal area corresponding to the tumor. (d) The corresponding ADC map estimated from b = 50, 2000 s/mm^2 shows a hypointense area, confirming the presence of the lesion. Mean ADC in the lesion was 0.68 × 10^{-3} mm^2/s.

3. Results

3.1. Subject and lesion characterization

The final sample included 43 patients diagnosed with PCa. Median ± interquartile range PSA values were 7.0 ± 4.2 ng/dL. The median ± interquartile range area of the 43 lesions was 14 ± 7 mm^2. Thirty-five lesions were localized in the PZ, 5 in the CG and 3 involved both regions. Of the 43 lesions, 7 had a GS 3 + 3, 13 GS 3 + 4, 15 GS 4 + 3, 4 GS 4 + 4 and 4 GS 4 + 5. In the CG portion, 3 lesions were classified as GS 3 + 3, 1 GS 3 + 4 and 1 GS 4 + 4. In the PZ, lesions were classified as: 4 GS 3 + 3, 12 GS 3 + 4, 12 GS 4 + 3, 3 GS 4 + 4 and 4 GS 4 + 5. Three lesions localized between the 2 different zones were classified as GS 4 + 3. For 22 lesions, histological results were performed by prostatectomy (2 in the CG, 19 in the PZ and 1 in both areas). For the other 21 lesions histology was obtained from TRUS biopsy.

Fig. 1 illustrates a case of a 65-years-old patient with PCa and includes different types of images: T2-w (Fig.1a), DWI with a b-value of 50 s/mm^2 (Fig.1b), b-value of 2000 s/mm^2 (Fig.1c) and the corresponding ADC map (Fig.1d).

3.2. ADC values by tissue type

Mean ADC ranges for all prostate tissues in the different localizations are summarized in Table 1, considering the 35 b-value pairs studied.

For the combinations that included a minimum b-value of 0 s/mm^2, absolute ranges of mean ADC were higher for all the tissues, compared to when a higher minimum b-value was used.

Also, maximum b-values seemed to influence the range of ADC values. When maximum b-values increased, the range of absolute mean ADC values tended to decrease for all tissue types.

3.3. Diagnostic performance and mean ADC values

For all the 35 b-value combinations, AUC ranged from 90.0%–96.0%. For the best 15 b-value combinations having AUC > 95%, the ADC cut-offs and diagnostic performance in lesion discrimination are presented in Table 2.

The AUC ranged from 95.1% to 96% to separate PCa from normal tissue. The comparison between ROC curves showed no significant differences in AUC between the best b-value pairs ($p > 0.05$). In any case, from the best combinations, the b-value pair 50, 2000 s/mm^2 showed the highest AUC (96.0%). Using an ADC cut-off of 0.89 × 10^{-3} mm^2/s sensitivity, specificity and accuracy were 95.5%, 93.2% and 94.4%, respectively. Fig. 2 presents the ADC distribution for normal (including peripheral zone and central gland) and malignant tissue for the b-value combination 50, 2000 s/mm^2 and corresponding ADC cut-off value used to separate PCa from normal tissue.

A detailed analysis of ADC values for normal tissue by region and PCa lesion localization for the 15 best b-value pair combinations is shown in Table 3. For all b-value combinations, mean ADC values showed significant differences between normal tissue and PCa globally ($p < 0.001$), in the PZ region ($p < 0.001$) and in the CG region ($p < 0.001$).

According to the performed Friedman test, mean ADC values for PCa and normal tissue were significantly different between the best b-

Table 1
Summary of mean ADC ranges for normal and PCa tissues for the 35 b-value combinations studied globally and by prostate region.

b-value pairs (s/mm^2)	ADC in PCa ($\times 10^{-3}$ mm^2/s)			ADC in Healthy tissue ($\times 10^{-3}$ mm^2/s)		
	Global	PZ	CG	Global	PZ	CG
All 35 studied combinations	0.56–1.32	0.56–1.33	0.53–1.26	0.81–1.74	0.81–1.89	0.80–1.74
bmin = 0	0.75–1.32	0.75–1.33	0.71–1.26	1.07–1.87	1.08–1.89	1.03–1.74
bmin > 0	0.56–1.16	0.56–1.17	0.53–1.08	0.81–1.68	0.81–1.70	0.80–1.55
bmax ≤ 1100	0.76–1.32	0.77–1.32	0.70–1.26	1.15–1.87	1.16–1.89	1.08–1.74
bmin = 0;bmax ≤ 1100	1.01–1.32	1.02–1.33	0.96–1.26	1.48–1.87	1.49–1.89	1.38–1.74
bmin > 0;bmax ≤ 1100	0.76–1.16	0.77–1.17	0.70–1.08	1.15–1.68	1.16–1.70	1.08–1.55
bmax ≥ 1100	0.56–1.01	0.56–1.02	0.53–0.96	0.81–1.48	0.81–1.49	0.80–1.38
bmin = 0;bmax ≥ 1100	0.75–1.01	0.75–1.02	0.71–0.96	1.07–1.48	1.08–1.49	1.03–1.38
bmin > 0;bmax ≥ 1100	0.56–0.93	0.56–0.94	0.53–0.86	0.81–1.38	0.81–1.39	0.80–1.28

bmin lowest b-value in the pair; *bmax* highest b-value in the pair; *ADC* apparent diffusion coefficient; *CG* central gland; *PZ* peripheral zone.
For example: bmin > 0;bmax ≤ 1100 includes all the combinations for which bmin is higher than 0 s/mm^2 and bmax is lower or equal to 1100 s/mm^2.

Table 2
Best b-value pair combinations with AUC > 95%, respective ADC cut-offs and diagnostic performance. The b-value combination with highest AUC is highlighted in bold.

Best b-value combinations (s/mm^2)	AUC	ADC cut-off ($\times 10^{-3}$ mm^2/s)	Diagnostic performance (%)		
			Sensitivity	Specificity	Accuracy
50,800	95.1	1.28	88.6	90.9	89.8
150,800	95.1	1.21	86.4	90.9	88.7
50,1100	95.1	1.18	90.9	88.6	89.8
0,1400	95.2	1.11	86.4	90.9	88.7
50,1400	95.5	1.05	88.6	90.9	89.8
100,1400	95.1	1.02	86.4	90.9	88.7
150,1400	95.1	1.00	88.6	90.9	89.8
0,1700	95.4	1.00	88.6	90.9	89.8
50,1700	95.5	0.93	88.6	95.5	92.1
100,1700	95.1	0.92	88.6	90.9	89.8
0,2000	95.9	0.96	93.2	90.9	92.1
50,2000	**96.0**	**0.89**	**95.5**	**93.2**	**94.4**
100,2000	95.7	0.86	95.5	93.2	94.4
150,2000	95.5	0.82	90.9	90.9	90.9
200,2000	95.6	0.80	90.9	93.2	92.1

ADC Apparent diffusion coefficient, *AUC* Area under the curve.

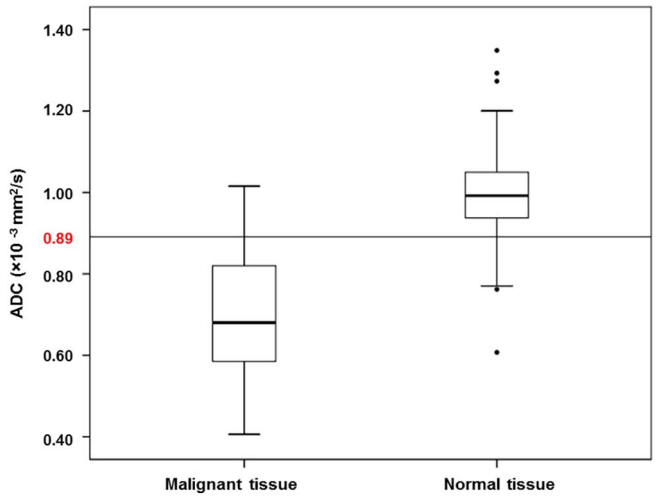

Fig. 2. Box plots for ADC values ($\times 10^{-3}$ mm^2/s) for healthy and malignant tissue for the combination of b = 50, 2000 s/mm^2. The horizontal line represents the corresponding ADC cut-off value for differentiating between normal and malignant tissues.

value pairs ($p < 0.001$), showing that the used b-values influence mean ADC results.

4. Discussion

The choice of b-values included in the DWI sequence is a central research issue, since it impacts the estimated ADC values [8,13,16,17]. Prostate studies focusing on specifically investigating the best b-value pair for ADC quantification at 3.0 T are still scarce [8,11,13,18]. Previous studies reported mean ADC values ranging from 0.65–1.15 $\times 10^{-3}$ mm^2/s in PCa and 0.96–1.79 $\times 10^{-3}$ mm^2/s for normal tissue [8,11,13,18]. In our study, globally, mean ADC values for PCa ranged from 0.56–1.32 $\times 10^{-3}$ mm^2/s and between 0.81 and 1.74 $\times 10^{-3}$ mm^2/s for normal tissue. Compared to the previously mentioned studies, our mean ADC ranges were similar for both PCa and normal tissue, although the observed ranges were slightly wider for both tissue types. Different factors could explain the difference in the mean ADC ranges between studies, namely variations in the physiological characteristics of the studied tissue types and localization of the lesions, PCa GS classification, differences in DWI protocols, including the choice of b-values and the methodology used in image analysis.

Our results demonstrate that PCa and normal tissue ADC values vary substantially with b-value combinations, in agreement with other studies. Previous ADC quantification studies used maximum b-values from 400 to 1000 s/mm^2 combined with b = 0 s/mm^2, reporting ADC in PCa between 0.71 and 1.87 $\times 10^{-3}$ mm^2/s and 1.03–3.71 $\times 10^{-3}$ mm^2/s in healthy tissue [8,13,16,17,19–21]. In our study, for similar combinations (maximum b-values between 500 and 1100 s/mm^2 combined with b = 0 s/mm^2), the range of ADC values for PCa was equivalent (1.01–1.32 $\times 10^{-3}$ mm^2/s). However, for both areas of normal glandular tissue (PZ and CG), the range and mean ADC values were lower than those previously reported [8,13,16,17,19].

For maximum b-values between 1000 and 2000 s/mm^2, combined with b = 0 s/mm^2, previous studies reported ADC values ranging from 0.65–0.88 $\times 10^{-3}$ mm^2/s for PCa and 1.07–1.44 $\times 10^{-3}$ mm^2/s for healthy tissue [7,11,18]. Comparable ADC ranges were found in our study for similar b-value combinations.

Other research groups used minimum b-values higher than b = 0 s/mm^2 and maximum b-values within 500–1000 s/mm^2, reporting PCa and normal tissue ADC ranging 0.79–1.5 $\times 10^{-3}$ mm^2/s and 1.39–2.7 $\times 10^{-3}$ mm^2/s, respectively. When testing similar b-value combinations, our results were similar for PCa, ranging 0.76–1.16 $\times 10^{-3}$ mm^2/s. However, in healthy tissue a lower maximum ADC value was obtained [22–24].

Overall, our results confirm that the estimated ADC is influenced by the used b-values. Using a minimum b-value higher than 0 s/mm^2 leads to lower ADC values. This was expected since including b = 0 s/mm^2 increases the contribution of micro-perfusion effects. This effect causes

Table 3
ADC values for PCa and normal tissue globally and by region for the b-value combinations with AUC > 95%, and corresponding *p*-values.

b-values (s/mm^2)	PCa ADC ($\times 10^{-3}$ mm^2/s)			Healthy tissue ADC ($\times 10^{-3}$ mm^2/s)			p-value* Global/PZ/CG
	Global	PZ	CG	Global	PZ	CG	
	Mean ± SD	Mean ± SD	Mean ± SD	Mean ± SD	Mean ± SD	Mean ± SD	
50,800	1.02 ± 0.22	1.04 ± 0.22	0.95 ± 0.20	1.52 ± 0.24	1.54 ± 0.24	1.41 ± 0.21	$p < 0.001/p < 0.001/p < 0.001$
150,800	0.96 ± 0.21	0.98 ± 0.21	0.89 ± 0.21	1.47 ± 0.24	1.48 ± 0.24	1.36 ± 0.21	$p < 0.001/p < 0.001/p < 0.001$
50,1100	0.93 ± 0.19	0.94 ± 0.19	0.86 ± 0.15	1.38 ± 0.20	1.39 ± 0.20	1.28 ± 0.18	$p < 0.001/p < 0.001/p < 0.001$
0,1400	0.91 ± 0.18	0.92 ± 0.19	0.88 ± 0.12	1.35 ± 0.19	1.36 ± 0.19	1.24 ± 0.17	$p < 0.001/p < 0.001/p < 0.001$
50,1400	0.84 ± 0.17	0.85 ± 0.18	0.81 ± 0.13	1.26 ± 0.19	1.27 ± 0.19	1.16 ± 0.17	$p < 0.001/p < 0.001/p < 0.001$
100,1400	0.83 ± 0.17	0.84 ± 0.17	0.79 ± 0.13	1.24 ± 0.19	1.25 ± 0.19	1.14 ± 0.17	$p < 0.001/p < 0.001/p < 0.001$
150,1400	0.80 ± 0.17	0.81 ± 0.17	0.77 ± 0.13	1.21 ± 0.19	1.22 ± 0.19	1.12 ± 0.17	$p < 0.001/p < 0.001/p < 0.001$
0,1700	0.82 ± 0.15	0.83 ± 0.17	0.80 ± 0.10	1.18 ± 0.17	1.20 ± 0.17	1.05 ± 0.14	$p < 0.001/p < 0.001/p < 0.001$
50,1700	0.77 ± 0.15	0.77 ± 0.16	0.73 ± 0.12	1.12 ± 0.17	1.13 ± 0.17	1.05 ± 0.14	$p < 0.001/p < 0.001/p < 0.001$
100,1700	0.75 ± 0.15	0.76 ± 0.15	0.72 ± 0.12	1.10 ± 0.17	1.11 ± 0.17	1.03 ± 0.13	$p < 0.001/p < 0.001/p < 0.001$
0,2000	0.75 ± 0.13	0.75 ± 0.14	0.71 ± 0.08	1.07 ± 0.13	1.08 ± 0.13	1.03 ± 0.12	$p < 0.001/p < 0.001/p < 0.001$
50,2000	0.69 ± 0.13	0.70 ± 0.14	0.65 ± 0.10	1.01 ± 0.14	1.02 ± 0.14	0.97 ± 0.12	$p < 0.001/p < 0.001/p < 0.001$
100,2000	0.68 ± 0.13	0.69 ± 0.13	0.64 ± 0.10	0.99 ± 0.13	0.99 ± 0.13	0.95 ± 0.12	$p < 0.001/p < 0.001/p < 0.001$
150,2000	0.66 ± 0.12	0.67 ± 0.13	0.62 ± 0.10	0.97 ± 0.14	0.97 ± 0.14	0.93 ± 0.11	$p < 0.001/p < 0.001/p < 0.001$
200,2000	0.64 ± 0.12	0.65 ± 0.13	0.60 ± 0.10	0.94 ± 0.14	0.94 ± 0.14	0.91 ± 0.11	$p < 0.001/p < 0.001/p < 0.001$

ADC apparent diffusion coefficient; AUC area under the curve; SD standard deviation; PZ peripheral zone; CG Central Gland.
* *p*-value differences in mean ADC values between PCa and healthy tissue globally and by region.

substantial signal attenuation at low b-values which explain higher ADC values when including very low b-values [12]. Maximum b-values also influence the ADC estimates; previous studies also showed that increasing the maximum b-value leads to lower ADC values [25]. At higher b-values the signal loss due to micro-perfusion effects is completed and only diffusion effects remain returning lower ADC values. Moreover, at high b-values normal prostate tissue signal is suppressed, increasing lesion conspicuity; the most malignant part of the tumor, representing the region of highest restriction is highlighted, and lower ADC values are measured. Higher b-values are nevertheless associated with decreased SNR which could lead to underestimated ADC values and lower diagnostic performances [26]. Despite this loss in SNR, in our study the b-value pair with highest diagnostic performance was 50, 2000 s/mm^2, even though there were no significant differences when comparing the AUC between the 15 best b-value pairs. The combined use of a 3 T equipment and a 32 channel receiver coil increase the achievable SNR. This type of coil is not often available in the clinical setting, where 4 to 16 channel coils are more frequently used [7,8,11,13,17,18,21,24]. SNR is also influenced by the used TE and guidelines recommend a TE lower than 90 ms [27] as used in our study (TE 66 ms).

Another important issue under investigation is the number of b-values used for ADC quantification. Multiple b-values can be used to perform ADC measurements, impacting its accuracy and precision [7,10,22]. Using a higher number of b-values increases the confidence associated to the estimated ADC compared to when only two b-values are used. Nevertheless, the larger the number of b-values included in a DWI sequence, the longer its acquisition time. In our study, we chose to evaluate only b-value pairs to identify the smallest set of b-values that would enable accurate ADC quantification within the shortest possible acquisition time, for wider applicability in the clinical practice.

The diagnostic performance of prostate DWI relies on the established ADC cut-off. Our results were consistent with previous studies [10,11] showing ADC values lower in malignant lesions than in normal tissue and AUC ranging from 90% to 96% for all b-value pairs.

The b-value pair 50, 2000 s/mm^2 showed the highest AUC (96%); for an ADC cut-off of 0.89 $\times 10^{-3}$ mm^2/s, sensitivity, specificity and accuracy were 95.5%, 93.2% and 94.4%, respectively. Mean ADC values were 1.01 ± 0.14 (global), 1.02 ± 0.14 (PZ), 0.97 ± 0.12 (CG) $\times 10^{-3}$ mm^2/s for normal tissue, and 0.69 ± 0.13 (global), 0.70 ± 0.14 (PZ) and 0.65 ± 0.1 (CG) $\times 10^{-3}$ mm^2/s for PCa.

In a similar study at 1.5 T, Peng et al. used b-values of 0, 50, 200, 1500 and 2000 s/mm^2 in 8 different b-value combinations, achieving AUC between 88.0%–93.0%. The best AUC (93.0%) was achieved for the b-value pair 0, 1000 s/mm^2 and for the b-value pair 50, 2000 s/mm^2 AUC, sensitivity and specificity were 89%, 88.9% and 89.5%, respectively. In their study, AUC comparison also showed no differences between the best b-value combinations [10]. Comparing our results to theirs, for a similar b-value pair (0,1100 s/mm^2), a higher AUC (94.7%) was obtained. In addition, in our study, higher AUC (96% vs 89%), sensitivity (95.5% vs 88.9%) and specificity (93.2% vs 89.5%) were achieved when the b-value pair 50, 2000 s/mm^2 was used for ADC estimation. The differences found between studies could be due to a higher SNR available at 3.0 T and to the use of a 32 channel phased-array coil. According to Shah et al., the endorectal coils normally used at 1.5 T can achieve the same clinical accuracy as a pelvic phase array coil at 3.0 T, although ADC values can differ [28]. Nevertheless, pelvic phase-array coils are greatly advantageous regarding patient comfort.

Also, the ROI delineation methodology is likely to influence ADC estimates. Some authors use T2-w images for lesion demarcation, others the b = 0 s/mm^2 or DW images with higher b-values [8,10,11,13,23]. Our methodology for ROI demarcation was different from that used by Peng et al. [10]; they used T2-w images and copied the ROI to the DW images whereas we drew the ROI at b = 2000 s/mm^2 and propagated them to the other DW images. Since we included only the most restricted lesion area, likely to represent the most malignant part of the tumor, this is likely to explain the lower ADC values obtained. However, other factors could have contributed to the ADC differences found between studies, namely variations in glandular and stromal structure, differences in DWI protocols and patient population [29].

In our study, the prostate anatomy was divided into PZ and CG. The term CG is used in the literature to represent the aggregation of the 'transitional zone' and the 'central zone'. Since in prostate MRI the separation between these zones is difficult, the term CG can be adopted to avoid erroneous identification of lesion localization [29].

Our study has some limitations. Firstly, lesion ROI may not have accurately reflected histological tumor outline. Also, we have to consider that mean ADC values in PCa may have been overestimated. Some patients underwent MRI after TRUS biopsy, which could have altered the ADC values due to the presence of residual hemorrhagic components. Although, we did not control the time between biopsy and MRI, during image analysis we were alert to avoid areas of hemorrhage on T1-w and T2-w images. Kim et al. reported that the influence of blood on ADC measurements could be ignored [30]. We used the mono-

exponential model since it is widely implemented but several papers highlight the importance of employing bi-exponential, kurtosis or other more complex models for studying PCa [31,32]. Furthermore, our sample was small, especially the number of included malignant CG lesions, making the ADC values potentially less representative. Furthermore, we had to exclude 19 patients from the study, since no lesions were detected in the MP-MRI analysis. However, it is well known that MP-MRI does not have a 100% negative predictive value, especially in lesions classified with GS < 7 and smaller than 0.5 cm^3 [33]. In any case, only 7 of those patients were diagnosed with PCa within 6 months of scanning. The relatively large slice thickness (6 mm) could have limited detectability; partial volume effects could also potentially explain why only one lesion was detected per patient while PCa is typically multifocal.

To our knowledge this is the first paper that performed ADC analysis in PCa at 3.0 T, using a large combination of b-value pairs, with b-values higher than b = 1000 s/mm^2 and several minimum b-values higher than b = 0 s/mm^2.

4. Conclusion.

Although several b-value pairs presented statistically comparable AUC, the b-value combination with highest AUC was b = 50, 2000 s/mm2 with a sensitivity, specificity and accuracy of 95.5%, 93.2% and 94.4%, respectively. Future prostate cancer studies should validate this combination by investigating ADC correlation with the GS.

Conflicts of interest

None.

Acknowledgments

We thank Professor Sandra Alves, Department of Biostatistics, School of Health of Porto/Polytechnic Institute of Porto (ESS/IPP), Rua Dr. António Bernardino de Almeida 400, 4200-072 Porto, Portugal, for the assistance in statistical analysis.

References

[1] Mocikova I, Babela J, Balaz V. Prostate cancer - the role of magnetic resonance imaging. Biomed Pap Med Fac Univ Palacky Olomouc Czech Repub 2012;156(2):103–7.
[2] Pentyala S, Whyard T, Pentyala S, Muller J, Pfail J, Parmar S, et al. Prostate cancer markers: an update. Biomed Rep 2016;4(2):263–8.
[3] Bjurlin MA, Meng X, Le Nobin J, Wysock JS, Lepor H, Rosenkrantz AB, et al. Optimization of prostate biopsy: the role of magnetic resonance imaging targeted biopsy in detection, localization and risk assessment. J Urol 2014;192(3):648–58.
[4] Aydın H, Kızılgöz V, Tekin BO. Overview of current multiparametric magnetic resonance imaging approach in the diagnosis and staging of prostate cancer. Kaohsiung J Med Sci 2015;31(4):167–78.
[5] Rais-Bahrami S, Turkbey B, Grant KB, Pinto PA, Choyke PL. Role of multiparametric magnetic resonance imaging in the diagnosis of prostate cancer. Curr Urol Rep 2014;15(3):387.
[6] Basser PJ. Inferring microstructural features and the physiological. NMR Biomed 1995;8(7):333–44.
[7] Metens T, Miranda D, Absil J, Matos C. What is the optimal b value in diffusion-weighted MR imaging to depict prostate cancer at 3T? Eur Radiol 2012;22(3):703–9.
[8] Tamada T, Kanomata N, Sone T, Jo Y, Miyaji Y, Higashi H, et al. High b value (2,000 s/mm^2) diffusion-weighted magnetic resonance imaging in prostate cancer at 3 tesla: comparison with 1,000 s/mm^2 for tumor conspicuity and discrimination of aggressiveness. PLoS One 2014;9(5):1–8.
[9] Wu LM, Xu JR, Gu HY, Hua J, Chen J, Zhang W, et al. Usefulness of diffusion-weighted magnetic resonance imaging in the diagnosis of prostate cancer. Acad Radiol 2012;19(10):1215–24.
[10] Peng Y, Jiang Y, Antic T, Sethi I, Schmid-Tannwald C, Eggener S, et al. Apparent diffusion coefficient for prostate cancer imaging: impact of b values. Am J Roentgenol 2014;202(3):247–53.
[11] Wang X, Qian Y, Liu B, Cao L, Fan Y, Zhang JJ, et al. High-b-value diffusion-weighted MRI for the detection of prostate cancer at 3 T. Clin Radiol 2014;69(11):1165–70.
[12] Weinreb JC, Barentsz JO, Choyke PL, Cornud F, Haider MA, Macura KJ, et al. PI-RADS prostate imaging - reporting and data system: 2015, version 2. Eur Urol 2016;69(1):16–40.
[13] Manenti G, Nezzo M, Chegai F, Vasili E, Bonanno E, Simonetti G. DWI of prostate cancer: optimal b-value in clinical practice. Prostate Cancer 2014;2014:868269.
[14] Thoeny HC, Keyzer F. Extracranial applications of diffusion-weighted magnetic resonance imaging. Eur Radiol 2007;17(6):1385–93.
[15] Delong ER, Delong DM, Clarke-pearson DL, Carolina N. Comparing the areas under two or more correlated receiver operating characteristic curves: a nonparametric approach. Biometrics 2016;44(3):837–45.
[16] De Rooij M, Hamoen EHJ, Fütterer JJ, Barentsz JO, Rovers MM. Accuracy of multiparametric MRI for prostate cancer detection: a meta-analysis. AJR Am J Roentgenol 2014;202(2):343–51.
[17] Kim TH, Jeong JY, Lee SW, Kim CK, Park BK, Sung HH, et al. Diffusion-weighted magnetic resonance imaging for prediction of insignificant prostate cancer in potential candidates for active surveillance. Eur Radiol 2015;25(6):1786–92.
[18] Koo JH, Kim CK, Choi D, Park BK, Kwon GY, Kim B. Diffusion-weighted magnetic resonance imaging for the evaluation of prostate cancer: optimal B value at 3 T. Korean J Radiol 2013;14(1):61–9.
[19] Carbone SF, Pirtoli L, Ricci V, Carfagno T, Tini P, La Penna A, et al. Diffusion-weighted magnetic resonance diagnosis of local recurrences of prostate cancer after radical prostatectomy: preliminary evaluation on twenty-seven cases. Biomed Res Int 2014;2014:780816.
[20] Caivano R, Rabasco P, Lotumolo A, Cirillo P, D'Antuono F, Zandolino A, et al. Comparison between Gleason score and apparent diffusion coefficient obtained from diffusion-weighted imaging of prostate cancer patients. Cancer Invest 2013;31(9):625–9.
[21] Korn N, Kurhanewicz J, Banerjee S, Starobinets O, Saritas E, Noworolski S. Reduced-FOV excitation decreases susceptibility artifact in diffusion-weighted MRI with endorectal coil for prostate cancer detection. Magn Reson Imaging 2015;33(1):56–62.
[22] Thörmer G, Otto J, Reiss-Zimmermann M, Seiwerts M, Moche M, Garnov N, et al. Diagnostic value of ADC in patients with prostate cancer: influence of the choice of b values. Eur Radiol 2012;22(8):1820–8.
[23] Rosenkrantz AB, Triolo MJ, Melamed J, Rusinek H, Taneja SS, Deng F-M. Whole-lesion apparent diffusion coefficient metrics as a marker of percentage Gleason 4 component within Gleason 7 prostate cancer at radical prostatectomy. J Magn Reson Imaging 2015;41(3):708–14.
[24] Boesen L, Chabanova E, Løgager V, Balslev I, Thomsen HS. Apparent diffusion coefficient ratio correlates significantly with prostate cancer gleason score at final pathology. J Magn Reson Imaging 2014;42(2):446–53.
[25] Tamada T, Sone T, Jo Y, Yamamoto A, Ito K. Diffusion-weighted MRI and its role in prostate cancer. NMR Biomed 2014;27(1):25–38.
[26] Jie C, Rongbo L, Ping T. The value of diffusion-weighted imaging in the detection of prostate cancer: a meta-analysis. Eur Radiol 2014;24(8):1929–41.
[27] Barentsz JO, Richenberg J, Clements R, Choyke P, Verma S, Villeirs G, et al. ESUR prostate MR guidelines 2012. Eur Radiol 2012;22(4):746–57.
[28] Shah ZK, Elias SN, Abaza R, Zynger DL, DeRenne LA, Knopp MV, et al. Performance comparison of 1.5-T endorectal coil MRI with 3.0-T nonendorectal coil MRI in patients with prostate cancer. Acad Radiol 2015;22(4):467–74.
[29] Jafar MM, Parsai A, Miquel ME. Diffusion-weighted magnetic resonance imaging in cancer: reported apparent diffusion coefficients, in-vitro and in-vivo reproducibility. World J Radiol 2016;8(1):21–49.
[30] Kim CK, Park BK, Lee HM, Kwon GY. Value of diffusion-weighted imaging for the prediction of prostate cancer location at 3 T using a phased-array coil: preliminary results. Invest Radiol 2007;42(12):842–7.
[31] Jambor I, Merisaari H, Aronen HJ, Järvinen J, Saunavaara J, Kauko T, et al. Optimization of b-value distribution for biexponential diffusion-weighted MR imaging of normal prostate. J Magn Reson Imaging 2014;39(5):1213–22.
[32] Jambor I, Merisaari H, Taimen P, Boström P, Minn H, Pesola M, et al. Evaluation of different mathematical models for diffusion-weighted imaging of normal prostate and prostate cancer using high b-values: a repeatability study. Magn Reson Med 2014;73(5):1988–98.
[33] Dianat SS, Carter HB, Macura KJ. Performance of multiparametric magnetic resonance imaging in the evaluation and management of clinically low-risk prostate cancer. Urol Oncol 2014;32(1):1–10.